

Science & Tech. of  
Nanostructured Mag.  
Materials  
NATO ASI Series 254  
497 (1991)

## ULTRAFINE MAGNETIC PARTICLES

G. C. Hadjipanayis, S. Gangopadhyay, L. Yiping

University of Delaware  
Department of Physics and Astronomy  
Newark Delaware 19716

C. M. Sorensen and K. J. Klabunde

Kansas State University  
Department of Physics  
Manhattan, Kansas 66506

### I. INTRODUCTION

Fine magnetic particles are scientifically and technologically very important. The particles are of great scientific interest in developing a better understanding of magnetic phenomena. From the technological point of view, they find wide applications in many types of materials including magnetic tapes, ferrofluids, catalysts, medical diagnostics, drug delivery systems, and pigments in paints and ceramics.<sup>1,2</sup> Magnetic particles are also found in the cells of some animals and in some bacteria which help them to navigate in geomagnetic fields.<sup>2</sup>

Research on fine magnetic particles started in late 1940's<sup>3,4</sup> and peaked in the 1950's. One of the milestones of that development was the emergence of domain theory<sup>5</sup> which led to the concept of single domain particles<sup>6</sup> and magnetic anisotropy contributions giving rise to permanent magnet behavior<sup>7</sup> and superparamagnetism.<sup>8</sup> More recently the potential application of fine magnetic particles in magnetic recording media<sup>9</sup> has reactivated experimental and theoretical research in these systems. In Japan<sup>10</sup> a five year research and development project on ultrafine magnetic particles (UFM) has been supported by the government to obtain further basic knowledge and technology for utilizing UFMs as a new category of materials. Today fine particles are being used in magnetic recording media in the form of acicular  $\gamma$ -Fe<sub>2</sub>O<sub>3</sub>, cobalt-modified  $\gamma$ -Fe<sub>2</sub>O<sub>3</sub>, iron, chromium dioxide, iron nitride, and barium ferrite particles (for perpendicular recording materials). These particles are single domain and have high magnetization, large coercivity, narrow size distribution, good dispersibility and high mechanical strength to ensure a strong output and a low signal noise.

There are several techniques for the preparation of fine particles including chemical reduction<sup>7,11-14</sup>, thermal<sup>15</sup>, spark erosion<sup>16</sup>, aerosolization<sup>17</sup>, vapor deposition<sup>9,18,19</sup>

and sputtering<sup>20-22</sup>. Most of these studies so far have been made on transition metal based systems. Elongated Fe and Fe-Co fine particles ( $l/d > 10$  with  $l = 30$  nm) with  $H_c$  about 1000 Oe have been produced by electrodeposition into mercury.<sup>7</sup> A higher coercivity ( $\sim 2140$  Oe) has been obtained<sup>22</sup> in elongated, but coarser Fe particles ( $l/d \sim 65$ ,  $l \sim 130$  nm; produced by reducing goethite (FeOOH) particles with hydrogen gas). Reduction of transition metal ions by  $\text{NaBH}_4$  or  $\text{KBH}_4$  has been used<sup>11,12-14</sup> to prepare fine crystalline Fe, Fe-Co, Fe-Co-B and Fe-Ni-B particles having sizes in the range 10-100 nm with  $H_c \sim 200$ -1000 Oe and  $M_s \sim 100$ -140 emu/g, with the lower values corresponding to amorphous particles. Amorphous Fe-C particles with a size of 8.5 nm have been prepared by thermal decomposition of iron pentacarbonyl.<sup>15</sup> Spark erosion<sup>16</sup> was also used to prepare amorphous Fe(Co)-Si-B particles in the range 5 nm - 25  $\mu$ . Very recently, aerosol pyrolysis has been used to prepare fine iron-oxide and barium ferrite particles<sup>17</sup> with interesting magnetic properties. The latter particles have also been produced in glassy matrices.<sup>23</sup> Gas evaporation is the most widely used technique<sup>9,10</sup> for the production of fine particles with a size range between several nanometers to micrometers. With this technique, narrow size distributions can be achieved,<sup>18</sup> leading to coercivities as high as 1580 Oe and saturation magnetizations up to 200 emu/g<sup>24</sup> A similar behavior has also been observed in granular solids where crystalline Fe<sup>20,21</sup> and amorphous Fe-Si<sup>25</sup> fine particles have been embedded in insulating  $\text{SiO}_2$  and BN matrices by sputtering. In Fe- $\text{SiO}_2$  the room temperature coercivity was 1500 Oe reaching a value beyond 2500 Oe upon cooling to 4.2 K.<sup>20</sup> Sputtering onto sputter-etched polymer substrates has also been used<sup>22</sup> to prepare crystalline Fe, Fe-Co and amorphous Fe-B and Co-B particles.

The magnetic properties of fine particle prepared by different techniques have been found to be different from the bulk. In ultrafine indium particles quantum size effects were found to affect the spin paramagnetism of small particles leading to a saturating magnetic moment at relatively low fields.<sup>26</sup> The reports are controversial on the size dependence of magnetization. Luborsky et al<sup>27</sup> claimed that  $M_s$  of ultrafine Fe particles prepared by electrodeposition was invariant with size even for particles 1.5 nm in size, where 50% of the atoms are on the surface, indicating a complete ferromagnetic coupling. However, for most of the Fe-based particles studied, a thin oxide coating has been found to protect the metallic core from further oxidation. In these particles Tamura et al<sup>28</sup> found the hyperfine field coming from the interface Fe atoms to be about 8% larger than the value of bulk Fe, indicating a larger moment for the Fe interface atoms. A similar observation has been made by Shinjo et al<sup>29</sup> in Fe thin films. The possible presence of a nonmagnetic (dead) layer in the surface layers remains a controversial issue.<sup>30,31</sup> Berkowitz et al<sup>32</sup> postulated the existence of a non-magnetic layer of 0.6 nm to explain the dependence of  $M_s$  on particle size in  $\gamma\text{-Fe}_2\text{O}_3$  particles. However, as pointed out by Morrish et al<sup>33</sup> and Coey et al<sup>34</sup> the surface spin structure of fine particles is canted and this can account for their lower magnetization. The spontaneous magnetization and Curie temperature of  $\text{Fe}_{75}\text{Si}_{15}\text{B}_{10}$  alloys have been found to decrease monotonically from ribbons to particles with decreasing particle size.<sup>35</sup> Berkowitz and Walter<sup>35</sup> attributed this to differences in short range order with an increased number of metalloid atoms around the Fe sites in fine particles.

In the past three years we have developed and refined some techniques for preparation of fine magnetic particles in the size range 2-500 nm with reasonable particle size control. Extensive characterization studies have yielded some fundamental knowledge of magnetic behavior for such small particles, and have uncovered some novel, perhaps unexpected magnetic properties.

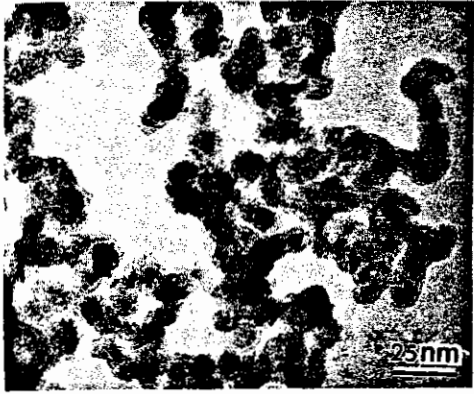


Figure 1. Bright field micrograph showing the morphology of Fe particles.

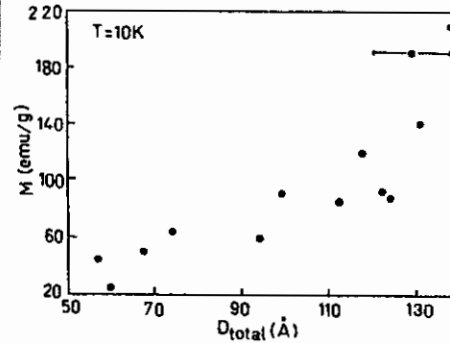


Figure 2. Magnetization as a function of particle size.

Throughout this work we have investigated two broad classes of materials: (1) Theories<sup>37</sup> and experiments have shown that the fluctuation of surface moments are larger than those of the interior so that  $B$  of the surface atoms is about 2-3.5 times larger than the interior. The problem, however, might be more difficult because of the possible lattice softening of the small particles<sup>38</sup> (and therefore softening of spin waves) and the geometrical size effect limiting the value of the spin wave wavelength.<sup>21</sup> Additional studies are needed to clarify this issue.

The smaller particles showed a superparamagnetic behavior with a blocking temperature,  $T_B$ , below 300 K. Above  $T_B$  no hysteresis was observed (Fig. 3a). The increase in  $H_c$  with particle size at 300 K is due to thermal effects observed in particles with size below the single domain particle size (Fig. 3a). At 10 K, thermal effects are negligible and a different behavior is observed;  $H_c$  decreases from 3400 Oe to  $\sim 1500$  Oe as the particle size is increased from 25 to 100 Å (Fig. 3b). The smallest particles had a coercivity of 3.4 kOe at 10 K, which decreased down to negligible values at 150 K, whereas the magnetization did not change drastically with temperature. At room temperature the maximum  $H_c$  was 900 Oe corresponding to a  $M_s$  of 150 emu/g and a corrected particle diameter of 11 nm. The strong temperature dependence of coercivity (Fig. 3c) is discussed later using Mössbauer spectroscopy.

The Mössbauer spectrum of an Fe sample with core diameter of 96 Å is shown in Fig. 4. Two magnetic hyperfine splitting patterns were found at a temperature of 85 K and below, which were attributed to  $\alpha$ -Fe and a mixture of  $\text{Fe}_3\text{O}_4$  and  $\gamma$ - $\text{Fe}_2\text{O}_3$ . Above 85 K a broad absorption band due to Fe-oxide is superimposed on the  $\alpha$ -Fe spectrum. The expected quadrupole splitting due to superparamagnetic particles was absent. Several explanations have been proposed to explain this behavior. Haneda et al<sup>38</sup> and Tamura et al<sup>28</sup> explained this broad absorption by assuming the existence of an asymmetrical uniaxial anisotropy in each Fe-oxide grains because of the presence of an unidirectional anisotropy due to the interaction with the metallic core. Because of this, the hyperfine field does not vanish even in the superparamagnetic state. The broad absorption band is explained by the distribution in the average hyperfine field because of the distribution in particle size. For

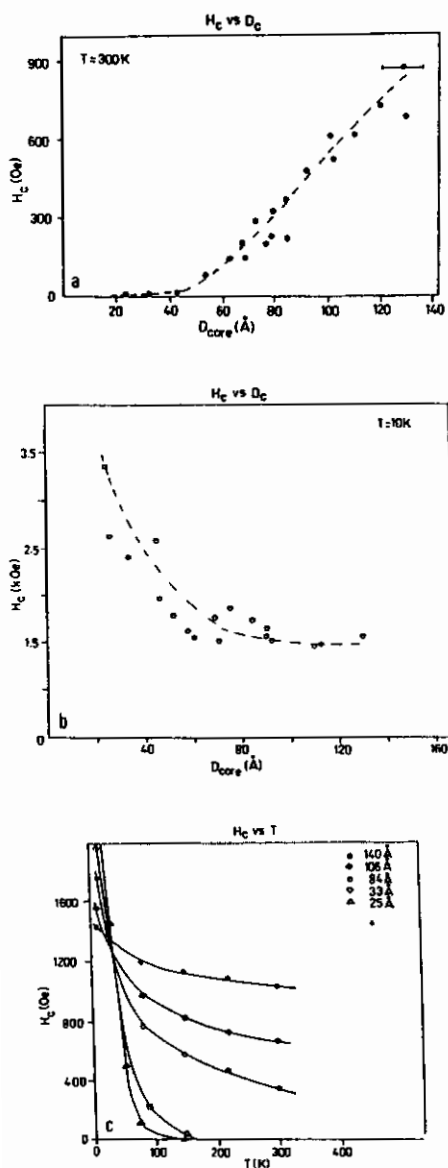


Figure 3. (a) Dependence of coercivity on particle size at  $T = 300\text{ K}$ . (b) Decrease in coercivity with increase in particle size at  $T = 10\text{ K}$  for Fe particles. (c) Temperature dependence of coercivity in Fe particles.

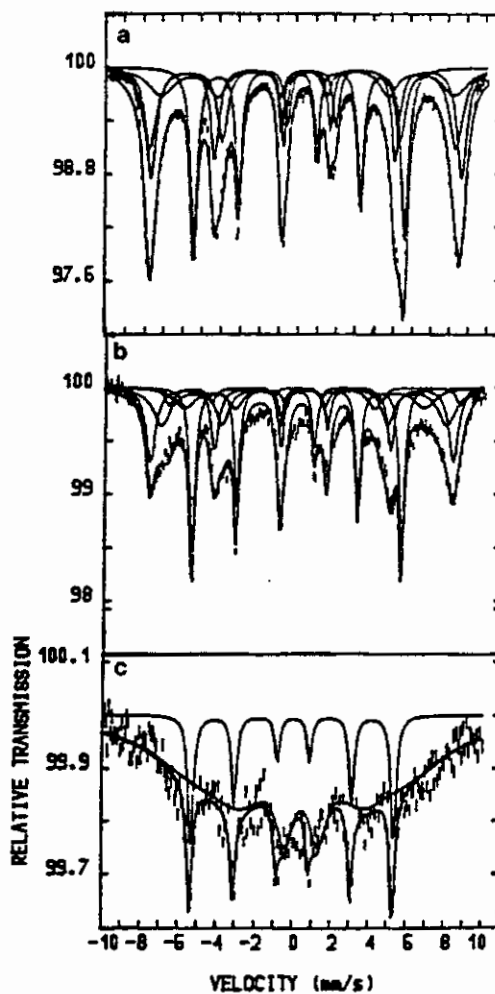


Figure 4. Mössbauer spectra in Fe particles with a size of  $96\text{ Å}$ , (a)  $T = 10\text{ K}$ , (b)  $T = 85\text{ K}$ , (c)  $T = 300\text{ K}$ .

Small metallic particles. In this work a critical feature with which we have spent considerable effort has been to develop chemical means of protection from oxidation. Without such protection small metallic particles are doomed to complete oxidation during study and/or use. (2) Small metal boride and oxide particles. In this work, in contrast to metallic particles, the challenge has been to develop means of obtaining desired particle sizes, morphologies, and chemical compositions.

So far our work has been very successful, both scientifically and technologically. We managed to produce fine Fe-based particles with high coercivities and unique properties which in most cases cannot be explained by existing models. In this article we will focus on the techniques of vapor deposition, reduction of metal ions and aerosolization.

## II. VAPOR DEPOSITION TECHNIQUES

### A. Fe-Smoke

In the evaporation-deposition technique, the deposition metal is vaporized in the presence of an inert gas. The metal vapors undergo collisions with the inert gas atoms resulting in vapor cooling, which causes a decrease in its mean free path leading to particle nucleation. Thereafter occurs the growth process which results in coagulation of the particles to form agglomerates which are then collected on a cold Cu substrate. Gas pressure below 10 torr results in the formation of fine particles with sizes of a few hundred angstroms.

We have studied in some detail the properties of fine Fe, Co and Ni particles prepared by evaporation in an Ar atmosphere at pressures in the range of 0.5 to 8.0 Torr. After deposition, the samples were subjected to a few hours soak in a diluted air-argon mixture to passivate their surface. The specimen was then removed to the atmosphere, weighed, and immobilized and sealed from further contact with the atmosphere by mixing with molten wax in a quartz capsule. In this paper we will concentrate only on Fe particles.

X-ray and selected area diffraction patterns (SAD) showed mostly the presence of  $\alpha$ -Fe lines and a few  $\text{Fe}_2\text{O}_3$  lines with the oxide lines being very diffuse.<sup>3</sup> The particle size measured from dark field micrographs was smaller than that of bright field indicating the presence of an oxide shell coating the metallic Fe core. This was further observed in bright field micrographs where rings of different contrast are seen around the core particles. Clusters of particles appeared in the electron micrographs when the deposits were sufficiently thick. No tendency for long chain formation was observed (Fig. 1). Most of the particles had nearly spherical shape with a total diameter in the range 5 - 20 nm. The core diameter range was 2.5-17 nm. This range falls in the single domain regime which for Fe is about 15 nm.<sup>6</sup>

The highest value of  $M_s$  was 200 emu/g for particles with an average size of 14 nm; this is 90% of the bulk value (220 emu/g). It was observed that as the particle size increased the apparent magnetization also increased (Fig. 2) because the oxide coating of constant thickness constituted a smaller fraction of the volume of larger particles. The temperature dependence of magnetization shows a common trend in all fine particles. For Fe fine particles,<sup>36</sup> the magnetization can be fitted to the  $BT^{3/2}$  law<sup>39</sup> predicted by the spin wave theory but with a value of the spin wave constant B much higher than in bulk Fe ( $B_{Fe} \sim 3.3 \times 10^{-6} \text{ K}^{2/3}$ ). Xiao and Chien<sup>21</sup> found a similar behavior in Fe granular solids with  $B \sim 4.5 \times 10^{-5} \text{ K}^{2/3}$ .

magnetic above 85 K, the sample as a whole shows an  $H_c$  of 507 Oe even at room temperature which increases to 1613 Oe at cryogenic temperatures where both the shell and the core show magnetic hyperfine splitting. When the oxide shell around the Fe core becomes superparamagnetic above 85 K, it affects the magnetization of Fe-core significantly through exchange interactions. In the smaller particles where the core is small enough, the fluctuation of the moment in the superparamagnetic oxide shell succeeds in making the whole particle soft. In the bigger particles, where the oxide-to-Fe ratio is much lower, the thermal fluctuations of the oxide moment are not strong enough to make the magnetic core magnetically soft and hence the coercivity is much higher at room temperature.

The coercivity of these Fe particles can not be explained by any of the existing models of magnetic hysteresis assuming the values of  $M_s$  and  $K$  for bulk Fe. These particles behave like they have a large effective anisotropy an order of magnitude higher than bulk Fe. We believe that the magnetic hysteresis properties are controlled by the nature and magnetic state of the surface layer and its interaction with the metallic Fe core.

### III. REDUCTION OF METAL IONS BY $\text{NaBH}_4$

Ultrafine transition metal boron particles were synthesized by reduction of metal salts with  $\text{NaBH}_4$  in aqueous solution.<sup>13,14,40</sup> Amorphous high boron content powders are usually produced by dropping the  $\text{NaBH}_4$  solution into the  $\text{FeCl}_3$  solution. However, if the two solutions are mixed in a Y-junction, a low B concentration powder is obtained which is also crystalline. The particle size can be varied by changing the concentration of solvent and solution. Normally a low concentration solution leads to larger particles. Also the use of ethanol instead of water leads to smaller particles because of the faster reaction rate.

The systems we have studied include Fe-B, Fe-Ni-B, Fe-Co-B and Co-B particles. First we studied the magnetic properties of Fe-B particles, then picked a particular Fe-B sample and gradually replaced Fe with Ni or Co to observe how the magnetic properties were changed. The magnetic and structural properties of these particles are briefly discussed below.

#### A. Fe-B particles

X-ray diffraction (XRD) patterns showed that the particles were amorphous for boron concentrations more than 20 at.%, otherwise they were crystalline. TEM showed that particles formed chainlike structures and their average monomer size ranged from 30 to 50 nm.  $H_c$  increased with decreasing particle size (Fig. 5). For a given size,  $H_c$  increased with increasing boron concentration, reached a maximum of more than 1000 Oe near 15 at.% B, and then decreased.  $M_s$  displayed the opposite behavior with a minimum value of about 60 emu/g. We believe this is due to the surface oxidation of these particles. As size decreases, the surface to volume ratio increases hence oxidation increases to yield smaller  $M_s$ . The oxidized layer enhances the effective surface anisotropy which yields larger  $H_c$ . At higher B concentration the particles became amorphous and this change in morphology caused  $H_c$  to drop while  $M_s$  increased.

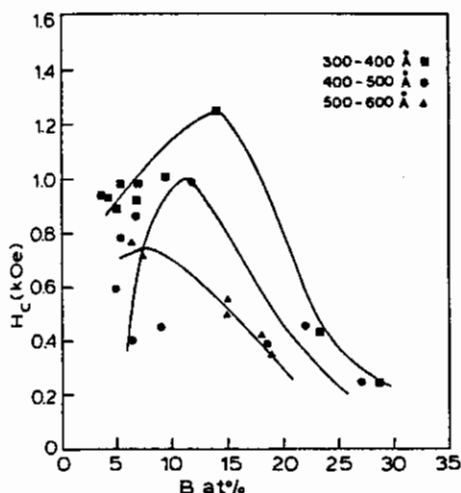


Figure 5. Coercivity of Fe-B particles versus the boron content.

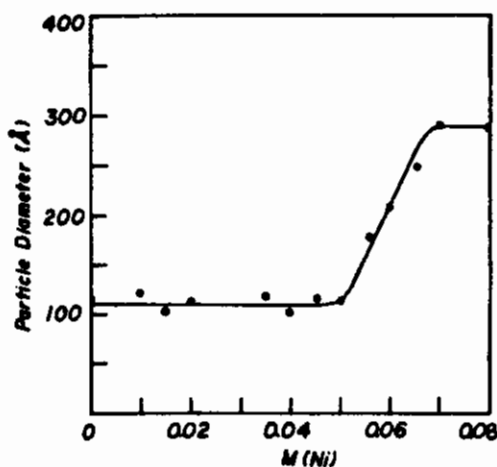


Figure 6. Particle size and boron content of Fe-Ni-B particles as a function of Ni molarity.

### B. Fe-Ni-B particles

For this study<sup>13</sup> we have chosen a Fe-B sample with Fe/B = 20 (at) which showed the largest  $H_c$  (1050 Oe). We then replaced Fe with Ni. Unfortunately, the boron concentration in the particles also changed (Fig. 6). Regardless of this, we studied the magnetic properties as a function of nickel salt molarity,  $M(\text{Ni})$ , of the solutions used to make the particles. XRD patterns showed that the particles became amorphous when  $M(\text{Ni}) \geq 0.05$  M and at the same time the particle size increased from a constant value of 10 nm to 30 nm for  $M(\text{Ni}) > 0.07$  M.  $H_c$  at 10 K showed an initial increase, reached a maximum of about 1550 Oe for  $M(\text{Ni}) = 0.015$  M, then decreased for higher  $M(\text{Ni})$  (Fig. 7). We concluded that a small amount of Ni addition into the Fe-B system increased the magnetic anisotropy and that caused  $H_c$  to increase.  $M_s$  data showed a monotonic decrease for the range  $M(\text{Ni}) = 0$  to 0.07 M. After that, it sharply dropped to almost zero. At higher boron concentrations Ni-B becomes nonmagnetic.

### C. Fe-Co-B

Fine Fe-Co-B particles were produced by a two step procedure. First, a 0.8M  $\text{NaBH}_4$  aqueous solution was added dropwise to a 0.4M mixed  $\text{FeCl}_3$  and  $\text{CoCl}_2$  aqueous solution while the pH value of the solution was kept at 8. The black precipitates were rinsed with distilled water and acetone, and dried in an Ar atmosphere chamber.

All the as-made powders were amorphous except those with boron content lower than 10 at%. With varying Fe:Co ratio, the amount of boron was found to vary in the range 5-30 at%. The dependence of Co and B content and particle size on the Fe:Co ratio is shown in Fig. 8. The particle size obtained was in the range of 20-30 nm. The saturation magnetization of as-made powders was relatively low, with a

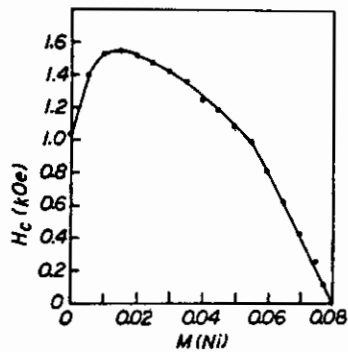


Figure 7. Coercivity as a function of Ni concentration.

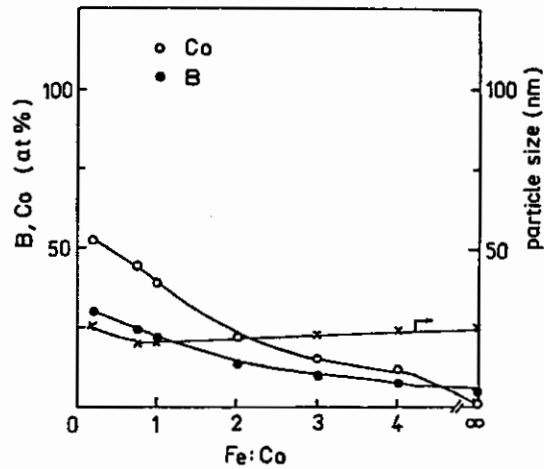


Figure 8. Dependence of chemical composition and particle size on Fe:Co ratio in Fe-Co-B particles.

maximum value of about 90 emu/g. A coercivity of about 1100 Oe at 300 K was found in an as-made crystalline sample with boron content of about 10 at%.

The magnetic properties of amorphous and crystallized isolated particles as a function of Fe:Co ratio are shown in Fig. 9. The maximum saturation magnetization obtained is 160 emu/g for a sample made with Fe:Co=4 which corresponds to 10 at% B. This is much different from bulk Fe-Co alloys where the maximum was obtained at 30 at% Co,<sup>9</sup> but similar to the Nd-Fe(Co)-B alloys where the maximum is about 12 at% Co.<sup>41</sup> The saturation magnetization of any composition corresponds to 75-80% of that of bulk iron-cobalt alloys. The other 20% is probably an oxide, but none of the oxide peaks were detected by X-ray diffraction may be because they are too broad and difused. The maximum coercivities obtained for the isolated particles were 1655 Oe at 10 K in a 25 at% Co powder, and 1940 Oe at 300 K in a 35 at% Co sample. The maximum coercivity is shifted to Co-rich powders when the temperature is increased from 10 K to 300 K.

The coercivity as a function of temperature for both annealed isolated and pressed particles is shown in Fig. 10. An anomalous behavior is observed with the temperature coefficient of coercivity depending on the Fe:Co ratio. When the powders contain only one transition metal, such as Fe-B, CoB<sup>14</sup> the temperature coefficient of coercivity is negative, with the coercivity at low temperatures being greater than that at higher temperatures. However, when the powders contain both Fe and Co, regardless of composition, the coefficient gradually changes to positive as shown in Fig. 10. The temperature coefficient of coercivity in pressed powders is always found to be negative with different ratio of Fe:Co similar to that for most bulk magnets.<sup>9</sup>

In summary, these systems display a wide variety of phenomena. Oxide layers seem to be more important in the iron systems. Co and perhaps Ni have poor magnetic properties until annealed to stoichiometric or crystalline phases. Most likely two differnt sources of anisotropy and hence  $H_c$  are involved. Future work



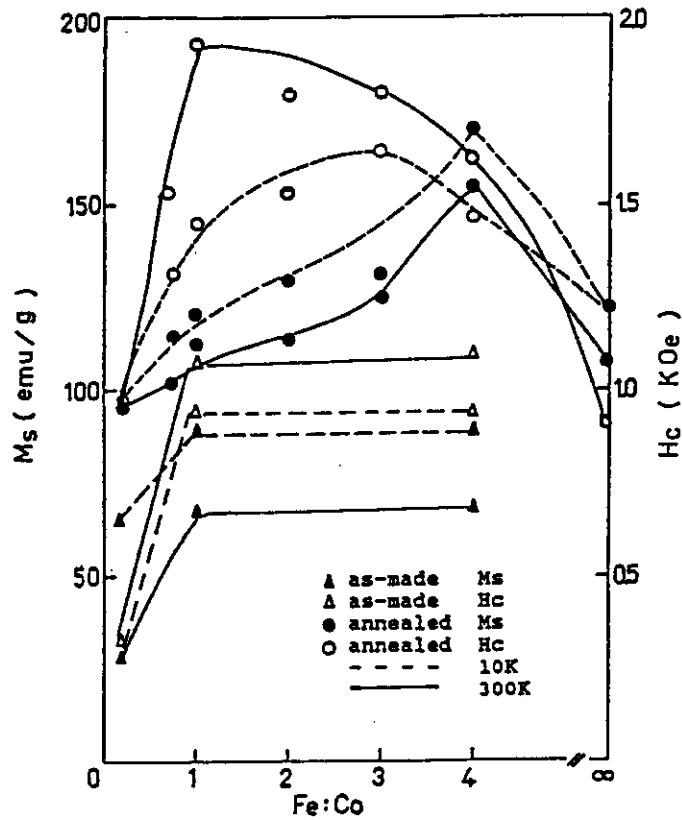


Figure 9. Magnetic properties of amorphous and crystallized Fe-Co-B particles.

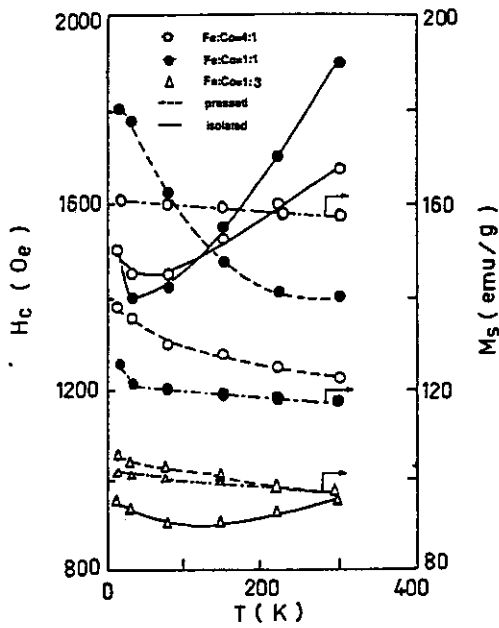


Figure 10. Coercivity of annealed Fe-Co-B particles as a function of temperature.

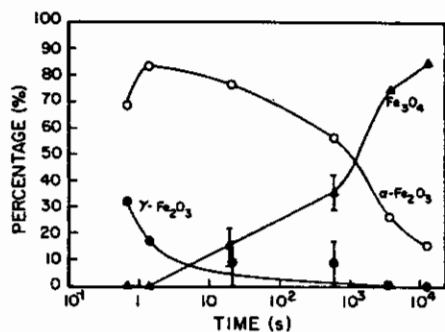


Figure 11. Phase formation in aerosol sprayed iron oxide particles.

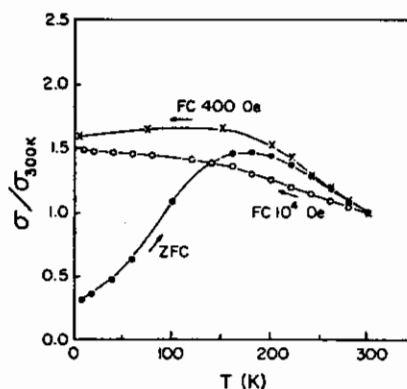


Figure 12. Thermomagnetic data in as-made barium ferrite particles showing a spin-glass type behavior.

will be concerned with comparing these systems further and controlling the surface chemical features.

#### IV. AEROSOL SPRAY PYROLYSIS

By aerosolizing, drying and baking aqueous solutions of pure and mixed metal salts, we can create nearly any metal oxide or mixed metal oxide particles conceivable.<sup>42,43</sup> An aerosol generator was used<sup>17</sup> to synthesize the fine particles from aqueous solutions of pure and mixed metal salts. The solution was fed to a constant output atomizer (Model 3075, TSI, St. Paul, MN) operated by a nitrogen gas flow of 2.6L/min at a pressure of 35 psi. The liquid drop aerosol stream passed through a diffusion dryer to remove water and then was heated to 800°C as it passed through a tube furnace. The aerosol particles were collected on cover glasses by thermophoresis after they passed through the tube furnace. Powder samples were obtained by scraping the particles off the cover glasses. Further heat treatment was also made in a nitrogen environment at 800°C.

##### A. Iron Oxides

Iron oxide particles with median diameter about 100 nm were created by spray pyrolysis of  $\text{Fe}_2(\text{SO}_4)_3$  solutions.<sup>44,17</sup> The phases produced could be changed from  $\gamma$  to  $\alpha$ - $\text{Fe}_2\text{O}_3$  to  $\text{Fe}_3\text{O}_4$  by heating in either air or  $\text{N}_2$  (Fig. 11). The magnetic properties of the particles directly followed from the phases present and their bulk properties. This project developed our technique and demonstrated the importance of the diffusion drier, without which the particles were hollow spheres.

##### B. $\text{BaO} \cdot 6\text{Fe}_2\text{O}_3$

Barium ferrite was created from an aqueous solution of Ba and  $\text{Fe}^{3+}$  nitrates. A novel phase was found in the as-received samples. These spherical particles were

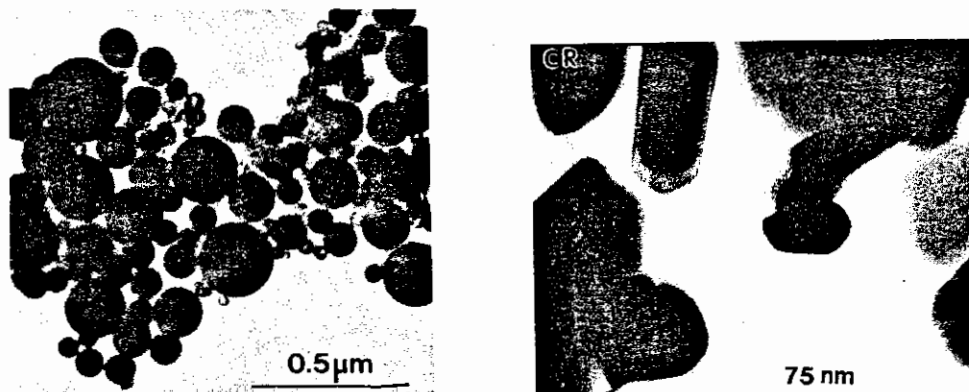


Figure 13. Structure morphology of amorphous and crystallized barium ferrite particles.

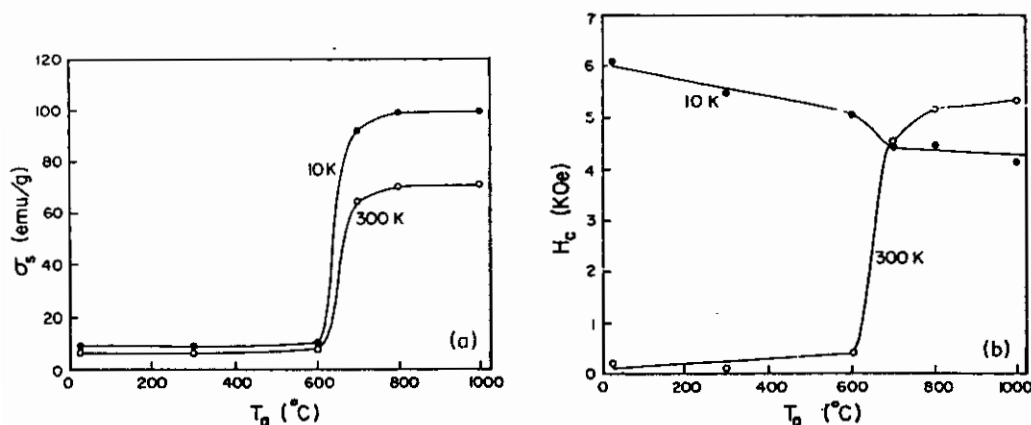


Figure 14. Magnetic properties of crystallized barium ferrite particles.

amorphous with a diameter about 100 nm and displayed a spin glass behavior (Fig. 12). Upon annealing at 800  $^{\circ}\text{C}$ , the sample became crystalline, with hexagonal morphology (Fig. 13) and the usual bulk magnetic properties of barium ferrite (Fig. 14). This work demonstrated two important aspects of this spray prolysis techniques: (1) the ability to create mixed oxides using short times and low temperatures compared to standard, time consuming milling-sintering techniques; and (2) the small size allows for quick quenching into metastable states which in this case led to an heretofore unknown phase.

## CONCLUSIONS AND FUTURE DIRECTION

Our studies so far have been very successful. We have developed and refined several techniques for preparation of fine magnetic particles with a size in the range of 2-500 nm depending on the procedure. Extensive characterization studies have

yielded some fundamental knowledge of magnetic behavior for such small particles and have uncovered some novel, perhaps unexpected properties. We have produced magnetically hard Fe and Fe-B particles which possess an anisotropy and coercivity one to two orders of magnitude higher than in bulk. Most of the particles made are coated by a surface layer oxide which is very important technologically and theoretically. The magnetic state of the surface layer and its interaction with the metallic core are found to affect the magnetic properties of the particle significantly.

There is still much to be learned about magnetic effects in small particles. The nature and magnetic state of surface layers and their effect on the particles' anisotropy and magnetic hysteresis need to be clarified. There is also a great need for systematic studies in order to understand better the magnetic hysteresis behavior. In the past the oversimplified theories of single domain particle and fanning have been used to explain the coercivities of particles even though microstructure and magnetic properties did not support the idea. The hysteresis behavior of these particles is rather complex and can not be explained by existing models. Thus, a new approach to these problems is needed.

#### ACKNOWLEDGEMENTS

This work has been supported by NSF-CHE-9013930. We are grateful to Dr. Kostikas and his colleagues at Demokritos in Athens, Greece for the Mössbauer measurements.

#### REFERENCES

1. E. Matijevic, MRS Bulletin, Volume XIV, 19 (1989).
2. M. Ozaki, MRS Bulletin, Volume XIV, 35 (1989).
3. L. Neel, Compt. Rend. 224, 1550 (1947).
4. R. Steinitz, Powder Met. Bull. 3, 124 (1948).
5. C. Kittel, Revs. Modern Phys. 21, 541 (1949).
6. A. H. Morrish, "The Physical Principles of Magnetism", John Wiley, New York (1965).
7. F. E. Luborsky, J. Appl. Phys. 32, 1715 (1961).
8. C. B. Bean and J. D. Livingston, J. Appl. Phys., 30, 1205 (1959).
9. A. Tasaki, S. Tomiyana, S. Iida, J. J. Appl. Phys. 4, 707 (1965).
10. C. Hayashi, J. Vac. Sci. Technol. A5, 1375 (1987).
11. T. Miyahara and K. Wawakauri, IEEE Trans. Magn. MAG-23, 2877 (1987).
12. I. Dragieva, G. Gavrillov, D. Buchkovand, M. Slavcheva, J. Less Comm. Metals 67, 375 (1979).
13. S. G. Kim, J. R. Brock, J. Coll. Interf. Sci. 116, 431 (1987).

14. S. Nafis, G. C. Hadjipanayis, C. M. Sorensen and K. J. Klabunde, IEEE Trans. Mag. 25, 3641 (1989); and to appear in J. Appl. Physics.; L. Yiping, G. C. Hadjipanayis, C. M. Sorensen and K. J. Klabunde, J. Magn. Magn. Mat., 79, 321 (1989).
15. J. van Wonerghem, S. Morup, S. W. Charles, S. Welles and J. Villadsen, Phys. Rev. Lett. 55, 410 (1985).
16. A. E. Berkowitz, J. L. Walter and K. F. Wall, Phys. Rev. Lett. 49, 1484.
17. a. Z. X. Tang, S. Nafis, C. M. Sorensen, G. C. Hadjipanayis and K. J. Klabunde, J. Magn. Magn. Mat., 80, 285 (1989). b. Z. X. Tang, S. Nafis, C. M. Sorensen, G. C. Hadjipanayis and K. J. Klabunde, IEEE Tans. Magn., 25, 4236 (1989).
18. C. G. Granqvist and R. A. Buhrman, J. Appl. Phys. 47, 2200 (1976).
19. A. Tasaki, M. Oda, S. Kashu and C. Hayashi, IEEE Trans. Mag. MAG-15, 1540 (1979).
20. G. Xiao, C. L. Chien, J. Appl. Phys., 61, 3308 (1987).
21. G. Xiao, C. L. Chien, J. Appl. Phys., 51, 1280 (1987).
22. S. Ohnuma, Y. Nakanouchi, C. D. Graham and T. Masumoto, IEEE Trans. Magn. MAS-21, 2038 (1985); AMG-22, 1098 (1986). A. L. Oppergard, F. J. Darnell and H. C. Miller, J. Appl. Phys. 32, 1845 (1961).
23. L. C. Nanna, S. Arajs, E. E. Anderson, APS Bulletin, 34, 976 (1989).
24. Y. W. Du, J. Wu, H. Lu, T. Wang, Z. Q. Hiu, H. Tang and J. C. Walker, J. Appl. Phys. 61, 3314 (1987).
25. R. L. Hotz, A. S. Edelstein, C. R. Gossett, preprint.
26. F. Meier and P. Wyder, Phys. Rev. Lett., 30, 181 (1973).
27. F. E. Luborsky and P. E. Lawrence, J. Appl. Phys., 32, 2315 (1961).
28. I. Tamura and M. Hayashi, Surf. Sci. 146, 501 (1984).
29. T. Shinjo, T. Shigematsu, N. Hosaito, T. Iwasaki, T. Takai, Japan J. Appl. Phys. 21, L220 (1982).
30. A. S. Edelstein, B. N. Das, R. L. Holtz, N. C. Koon, M. Rubinstein, S. A. Wolf and K. E. Kihlstrom, J. Appl. Phys. 61, 3320 (1987).
31. A. Tasaki, M. Takao and H. Tokunaga, J. J. Appl. Phys. 13, 271 (1974).
32. A. E. Berkowitz, W. J. Schuele and P. J. Flanders, J. Appl. Phys. 39, 1261 (6C6), 301 (1987).
33. A. H. Morrish, K. Haneda and P. J. Schiurer, J. de Physique, C6, 301 (1976).
34. J. M. D. Coey and D. Khalafella, Phys. Stat. Sol. (A) 11, 229 (1972).

35. A. E. Berkowitz and J. L. Walter, *Mat. Sci. Eng.* **55**, 275 (1982).
36. S. Gangopadhyay, E. B. Dale, G. C. Hadjipanayis, C. M. Sorensen and K. J. Klabunde (in preparation).
37. D. L. Mills, *Comm. Solid State Phys.* **4**, 28 (1971).
38. K. Haneda and A. H. Morrish, *Nature*, **282**, 186 (1979).
39. C. Kittel, "Introduction to Solid State Physics," John Wiley, New York (1966).
40. S. Linderoth, S. Morup and M. D. Bentzon, *J. Magn. Mang. Mat.* **83**, 457 (1990).
41. Y. Maisuura, S. Hirosawa et al, *Appl. Phys. Lett.* **46**, 308 (1985).
42. T. T. Kodas, *Adv. Mat.* **180** (1989).
43. M. Ramamurthi and K. Leong, *J. Aerosol. Sci.* **18**, 175 (1987)
44. S. Nafis, Z. X Tang, E. B. Dale, C. M. Sorensen, G. C. Hadjipanayis and K. J. Klabunde, *J. Appl. Phys.* **64**, 5835 (1988).